

# FORETINIB

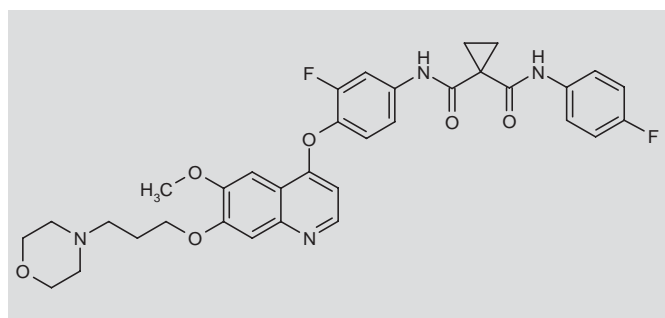
Rec INN; USAN

*c-Met and VEGFR-2 Inhibitor  
Oncolytic*

1363089  
EXEL-2880  
GSK-089  
GSK-1363089  
XL-880

*N*-[3-Fluoro-4-[6-methoxy-7-[3-(4-morpholinyl)propoxy]quinolin-4-yloxy]phenyl]-*N'*-(4-fluorophenyl)cyclopropane-1,1-dicarboxamide

InChI: 1S/C34H34F2N4O6/c1-43-30-20-25-27(21-31(30)45-16-2-13-40-14-17-44-18-15-40)37-12-9-28(25)46-29-8-7-24(19-26(29)36)39-33(42)34(10-11-34)32(41)38-23-5-3-22(35)4-6-23/h3-9,12,19-21H,2,10-11,13-18H2,1H3,(H,38,41)(H,39,42)



C<sub>34</sub>H<sub>34</sub>F<sub>2</sub>N<sub>4</sub>O<sub>6</sub>  
Mol wt: 632.6538  
CAS: 849217-64-7  
EN: 370259

## SUMMARY

The *c-Met* and vascular endothelial growth factor receptor (VEGFR) tyrosine kinases are activated in multiple cancer types and drive a variety of cancer-associated processes, including tumor cell proliferation, invasion, metastasis and angiogenesis. These receptor tyrosine kinases (RTKs) are therefore attractive therapeutic drug targets for a wide range of tumor types. Foretinib is a broadly specific tyrosine kinase inhibitor that targets a spectrum of RTKs, including *c-Met* and VEGFR-2. It has shown potent preclinical antitumor activity in the laboratory setting, primarily through the reduction of tumor growth and angiogenesis in animal models. Phase I trials have shown foretinib to

be well tolerated at clinically active levels when administered once daily on the first 5 days of a 14-day cycle, with the majority of treatment-related adverse responses reversed by either a scheduled break in treatment or a decrease in dose. The recommended dose has been defined as 240 mg and this dose is currently being used in phase II clinical trials in multiple tumor types following the same dosing regimen.

## SYNTHESIS\*

Foretinib can be obtained by the following synthetic strategies:

- Condensation of the phenolic compound (I) with 7-benzyloxy-6-methoxyquinolinyl triflate (II) in refluxing 2,6-lutidine affords the quinolinyl ether (III), which is *O*-debenzylated by transfer hydrogenation with 1,4-cyclohexadiene and Pd/C in EtOH at 65 °C, producing the 7-hydroxyquinoline derivative (IV). Finally, the hydroxyquinoline (IV) is alkylated with *N*-(3-chloropropyl)morpholine hydrochloride (V) by means of K<sub>2</sub>CO<sub>3</sub> in DMF at 90 °C (1, 2). Scheme 1.
- Direct coupling of the phenol derivative (I) with 4-chloro-6-methoxy-7-(3-morpholinopropoxy)quinoline (VI) in the presence of Pd(OAc)<sub>2</sub>, 2-(di-*tert*-butylphosphino)-1,1'-binaphthyl (DTBPB) and K<sub>3</sub>PO<sub>4</sub> in anisole at 110 °C or NMP/toluene at 95 °C (3). Scheme 1.
- Acylation of the quinolinyl oxyaniline intermediate (VII) with 1-(4-fluorophenyl)carbamoyl)cyclopropanecarbonyl chloride (VIII) by means of K<sub>2</sub>CO<sub>3</sub> in THF/H<sub>2</sub>O (4). Scheme 1.

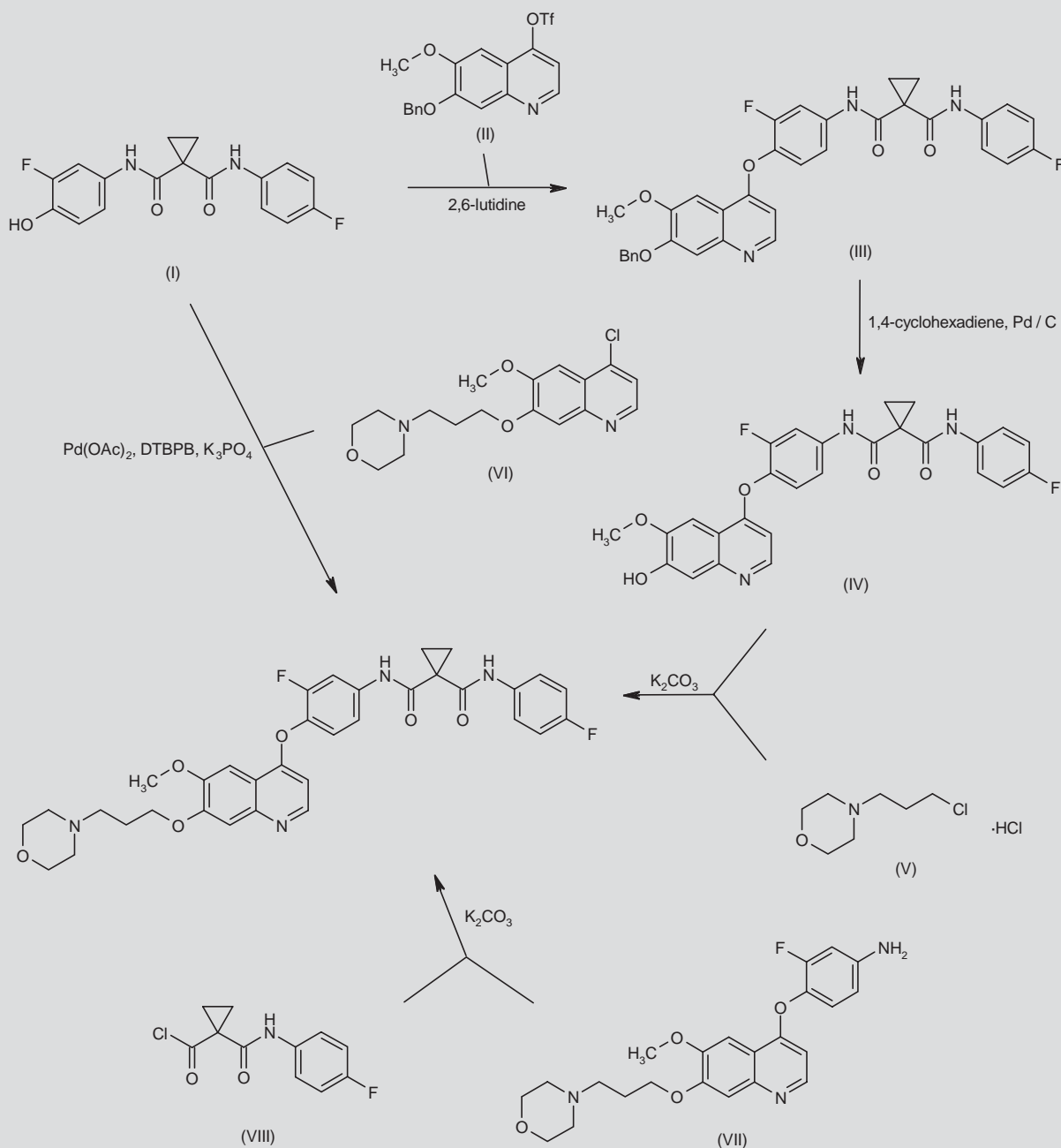
The precursors cyclopropane-1,1-bis(carboxamide) (I) and acid chloride (VIII) are prepared as follows:

Treatment of cyclopropane-1,1-dicarboxylic acid (IX) with one equivalent of SOCl<sub>2</sub> in the presence of Et<sub>3</sub>N in THF at 0 °C, followed by condensation of the activated intermediate with 4-fluoroaniline (X), provides the monoamide (XI) (1, 3, 4), which is optionally chlorinated to (VIII) by treatment with oxalyl chloride in cold THF (3, 4). Scheme 2.

K. Hedgethorpe and P.H. Huang. Protein Networks Team, Section of Cell and Molecular Biology, Institute of Cancer Research, 237 Fulham Road, London SW3 6JB, UK. E-mail: paul.huang@icr.ac.uk.

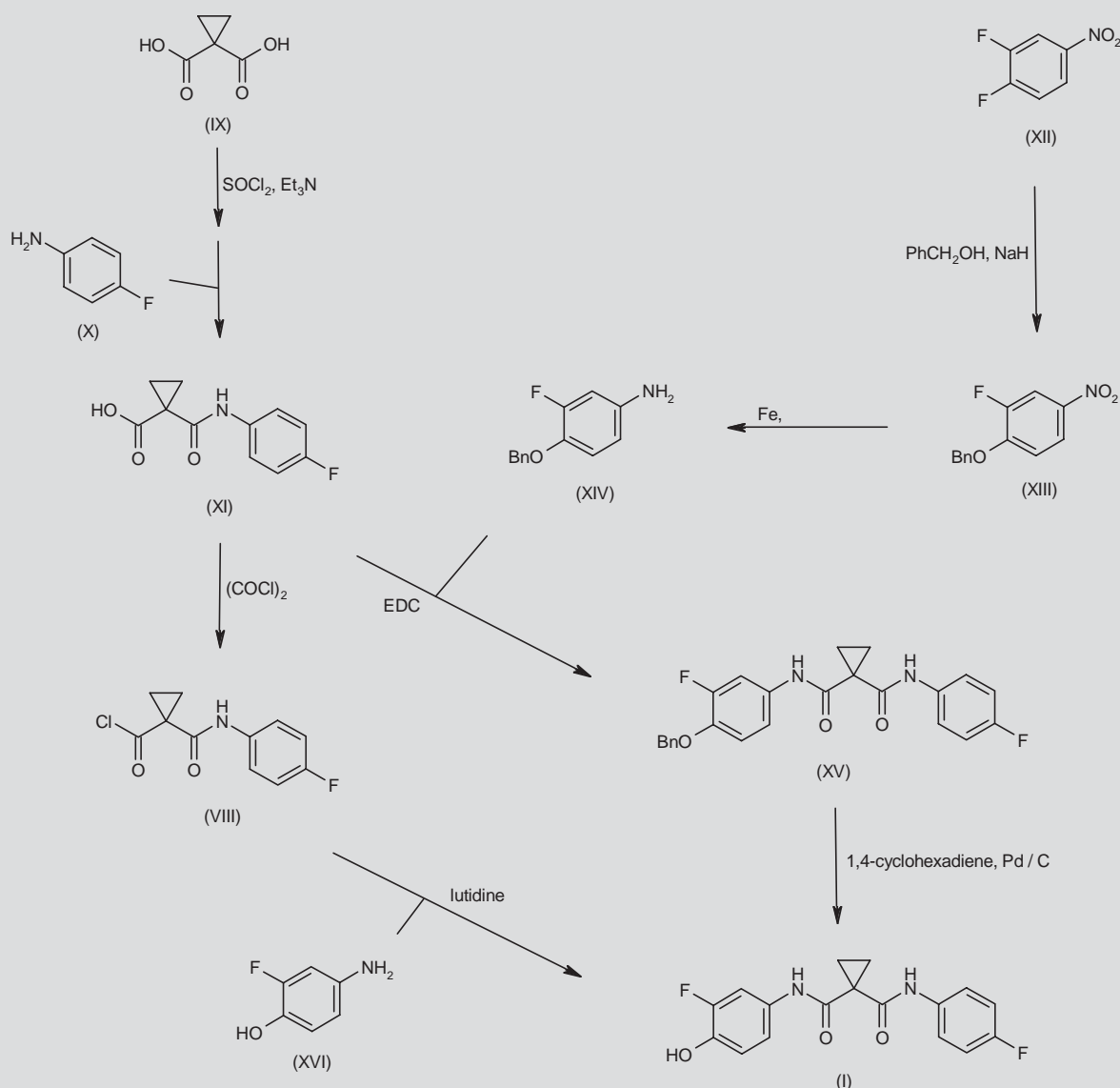
\*Synthesis prepared by R. Pandian, J. Bolòs, R. Castañer. Thomson Reuters, Provença 388, 08025 Barcelona, Spain.

### Scheme 1. Synthesis of Foretinib



Reaction of 3,4-difluoronitrobenzene (XII) with sodium benzoate—prepared from benzyl alcohol and NaH in dimethylacetamide—gives 1-benzyloxy-2-fluoro-4-nitrobenzene (XIII) as the main product. Subsequent reduction of compound (XIII) by means of iron and ammonium formate in refluxing toluene leads to the corresponding aniline (XIV), which is subsequently coupled with carboxylic acid (XI)

using EDC in  $\text{CH}_2\text{Cl}_2$  to afford the diamide (XV). Finally, debenzyla-  
tion of diamide (XV) by transfer hydrogenation with 1,4-cyclohexadi-  
ene and Pd/C in boiling EtOH provides the target intermediate (I) (1).  
Scheme 2. Alternatively, acid chloride (VIII) can be directly con-  
densed with 4-amino-2-fluorophenol (XVI) in the presence of 2,6-  
lutidine in cold THF to give diamide (I) (3). Scheme 2.

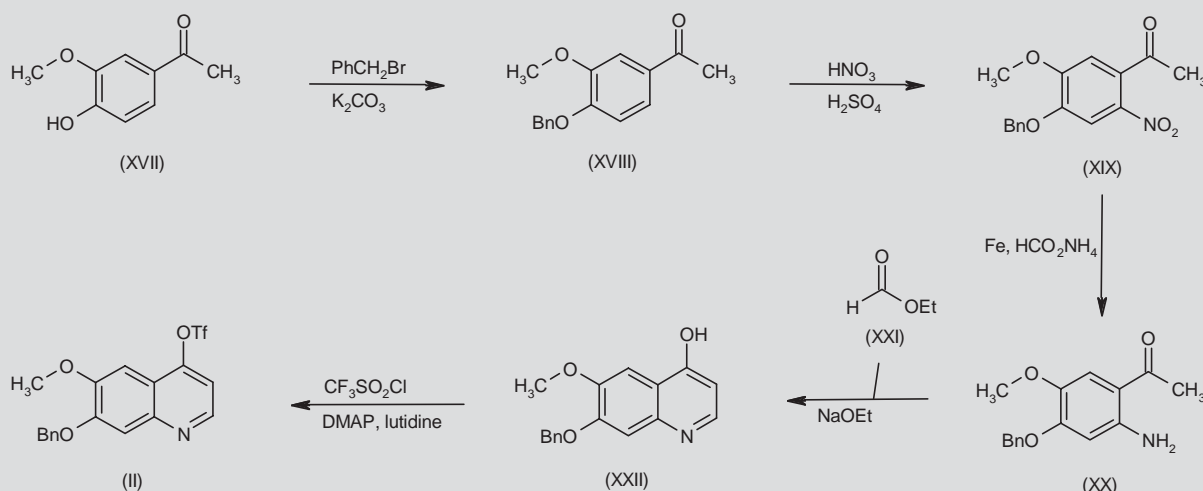
**Scheme 2.** Synthesis of Precursors (I) and (VIII)

Quinolinylnyl triflate (II) is obtained by the following method:

Alkylation of 4'-hydroxy-3'-methoxyacetophenone (XVII) with benzyl bromide by means of  $\text{K}_2\text{CO}_3$  in DMF gives benzyl ether (XVIII), which is reacted with fuming  $\text{HNO}_3$  and concentrated  $\text{H}_2\text{SO}_4$  in cold  $\text{CH}_2\text{Cl}_2$  to afford 4'-benzyloxy-5'-methoxy-2'-nitroacetophenone (XIX). After reduction of the nitro group of compound (XIX) using iron powder and ammonium formate in refluxing  $\text{H}_2\text{O}$ /toluene, the resulting 2-aminoacetophenone derivative (XX) cyclizes with ethyl formate (XXI) in the presence of  $\text{NaOEt}$  in DME, providing 7-benzyloxy-6-methoxy-4-quinolinol (XXII). Finally, quinolinol (XXII) is treated with trifluoromethanesulfonyl chloride in the presence of DMAP and 2,6-lutidine in cold  $\text{CH}_2\text{Cl}_2$  (1, 5). Scheme 3.

The 7-(morpholinopropoxy)quinoline (VI) intermediate can be prepared as follows:

Alkylation of 4'-hydroxy-3'-methoxyacetophenone (XVII) with 1-bromo-3-chloropropane (XXIII) in the presence of  $\text{K}_2\text{CO}_3$  and the phase-transfer catalyst  $\text{Bu}_4\text{NBr}$  in  $\text{H}_2\text{O}$  at  $80^\circ\text{C}$  affords a mixture of the chloropropoxy- and bromopropoxy-acetophenones (XXIVa) and (XXIVb) (3), which, without separation, are subjected to electrophilic nitration with aqueous  $\text{HNO}_3$  and  $\text{H}_2\text{SO}_4$  to give the corresponding nitro derivatives (XXVa) and (XXVb). Condensation of the halopropoxy compounds (XXVa) and (XXVb) with morpholine (XXVI) by means of  $\text{K}_2\text{CO}_3$ ,  $\text{NaI}$  and  $\text{Bu}_4\text{NBr}$  in toluene/ $\text{H}_2\text{O}$  at  $85^\circ\text{C}$  results in the morpholinopropoxy derivative (XXVII) (3, 4). Alternatively, inter-

**Scheme 3.** Synthesis of Quinoliny Triflate (II)

mediate (XXVII) can be prepared by treatment of 4'-hydroxyacetophenone (XVII) with 1,3-propanediol cyclic sulfate (XXVIII) in the presence of  $\text{LiOH}$  in boiling  $\text{H}_2\text{O}/\text{THF}$ , followed by reaction of the intermediate alkyl sulfate with morpholine (XXVI) to afford the 4'-(morpholinopropoxy)acetophenone (XXIX). Finally, subsequent nitration of acetophenone (XXIX) with  $\text{HNO}_3$  and TFA in  $\text{CH}_2\text{Cl}_2$  leads to intermediate (XXVII) (3). After reduction of the nitro group in compound (XXVII) by transfer hydrogenation with  $\text{HCOOH}/\text{HCOOK}$  in the presence of  $\text{Pd}/\text{C}$  in  $\text{H}_2\text{O}/\text{EtOH}$ , the obtained aminoacetophenone (XXX) is cyclized with ethyl formate (XXI) by means of  $\text{NaOEt}$  in  $\text{EtOH}/\text{toluene}$  to yield quinolinol (XXXI). Finally, quinolinol (XXXI) is chlorinated by means of  $\text{POCl}_3$  in acetonitrile at  $55^\circ\text{C}$  (3, 4). Scheme 4. Alternatively, chloroquinoline (VI) can be directly obtained by Vilsmeier reaction of aminoacetophenone (XXX) with *N*-methyl-*N*-phenylformamide (XXXII) and oxalyl chloride in dichloroethane at  $60^\circ\text{C}$  (3). Scheme 4.

The 4-(aminophenoxy)quinoline precursor (VII) can be obtained from chloroquinoline (VI) by two related methods. Condensation of chloride (VI) with 2-fluoro-4-nitrophenol (XXXIII) in 2,6-lutidine at  $140\text{--}145^\circ\text{C}$  affords the 2-fluoro-4-nitrophenyl ether (XXXIV), which is then reduced by catalytic hydrogenation over  $\text{Pd}/\text{C}$  in the presence of  $\text{HCl}$  in  $\text{H}_2\text{O}/\text{EtOH}$  (4). Scheme 5. Alternatively, by direct coupling of chloroquinoline (VI) with 2-fluoro-4-aminophenol (XVI) by means of sodium *tert*-butoxide in DMAc at  $100^\circ\text{C}$  (4). Scheme 5.

## BACKGROUND

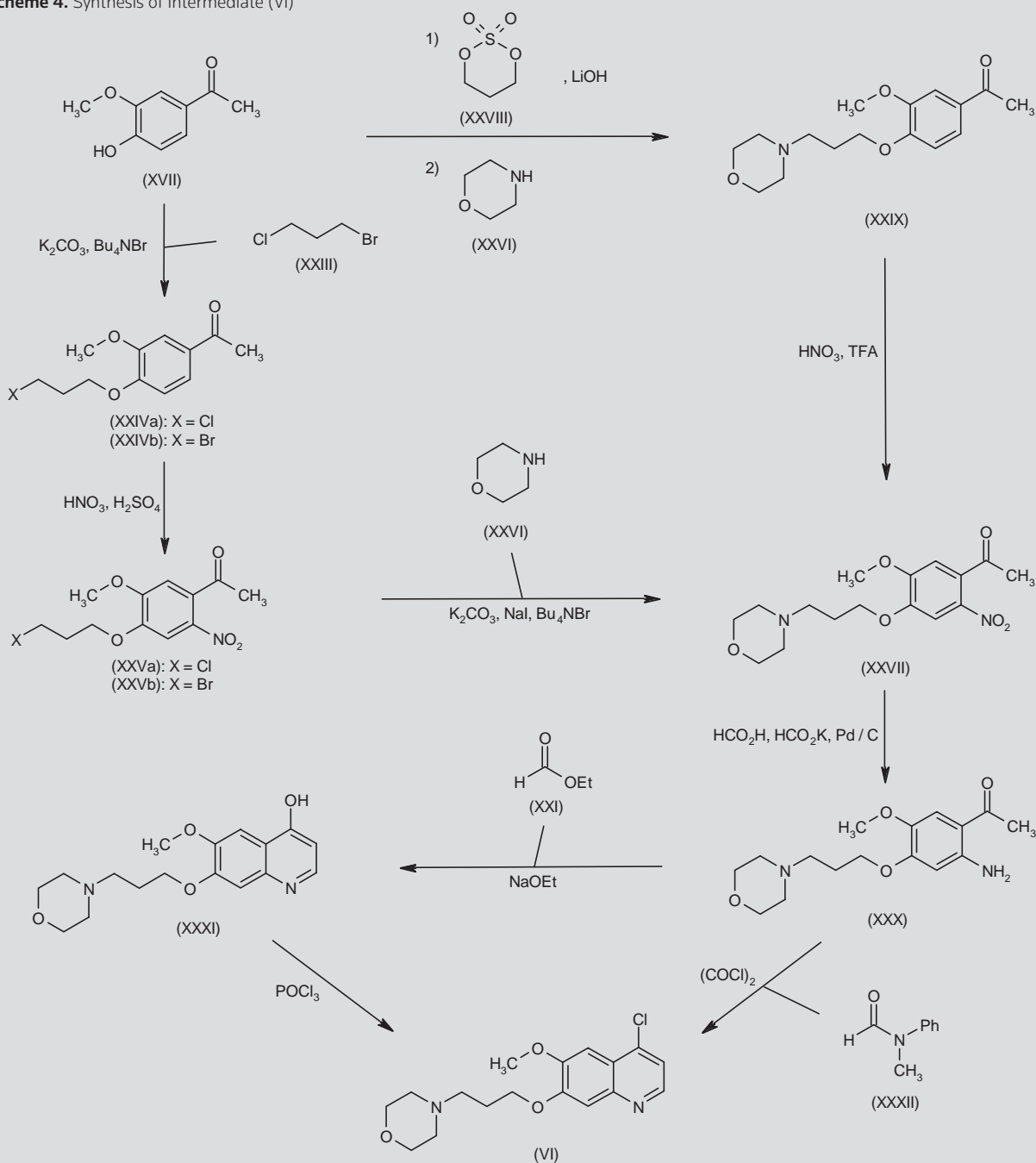
The receptor tyrosine kinase (RTK) c-Met is activated by binding to its ligand, hepatocyte growth factor (HGF), and is critical for regulating physiological processes, such as cell growth, survival and motility (6). Dysregulation of c-Met through either receptor overexpression or mutation leads to constitutive activation, which has been observed in a variety of human cancers, including papillary renal carcinoma (7), gastric carcinoma (8), small cell lung cancer (9) and

breast cancer (10). Many tumor cells with amplification of the *MET* gene are dependent upon it to maintain cell survival, a concept known as oncogene addiction (11). Inhibition of this receptor has been shown to result in apoptosis of these "addicted" cells. *MET* amplification and mutation are particularly prevalent in metastatic lesions, implicating them in the invasiveness and dissemination of tumors (12).

Vascular endothelial growth factor receptor 2 (VEGFR-2) is another RTK and a member of the VEGF receptor family. It is expressed on the surface of vascular endothelial cells and activated by the VEGF ligand (13). Expression of both VEGFR-2 and c-Met is upregulated as a result of tumor hypoxia, and these receptors cooperate to increase tumor cell invasiveness and drive angiogenesis (14). Additionally, both c-Met and VEGFR-2 upregulate the expression of VEGF-regulated genes, preventing endothelial apoptosis, promoting capillary formation *in vivo* and increasing the microvessel density in tumors (15, 16).

There is extensive crosstalk between RTKs, which results in the activation of common downstream signaling pathways (17). In a process known as "RTK coactivation", cancer cells often activate more than one RTK in order to achieve chemoresistance against single target agents through pathway compensation and network robustness (18). It is thought that broad-spectrum RTK inhibitors would make particularly effective therapeutic agents in comparison to single-target c-Met or VEGFR-2 inhibitors (19, 20) by shutting down compensatory survival pathways.

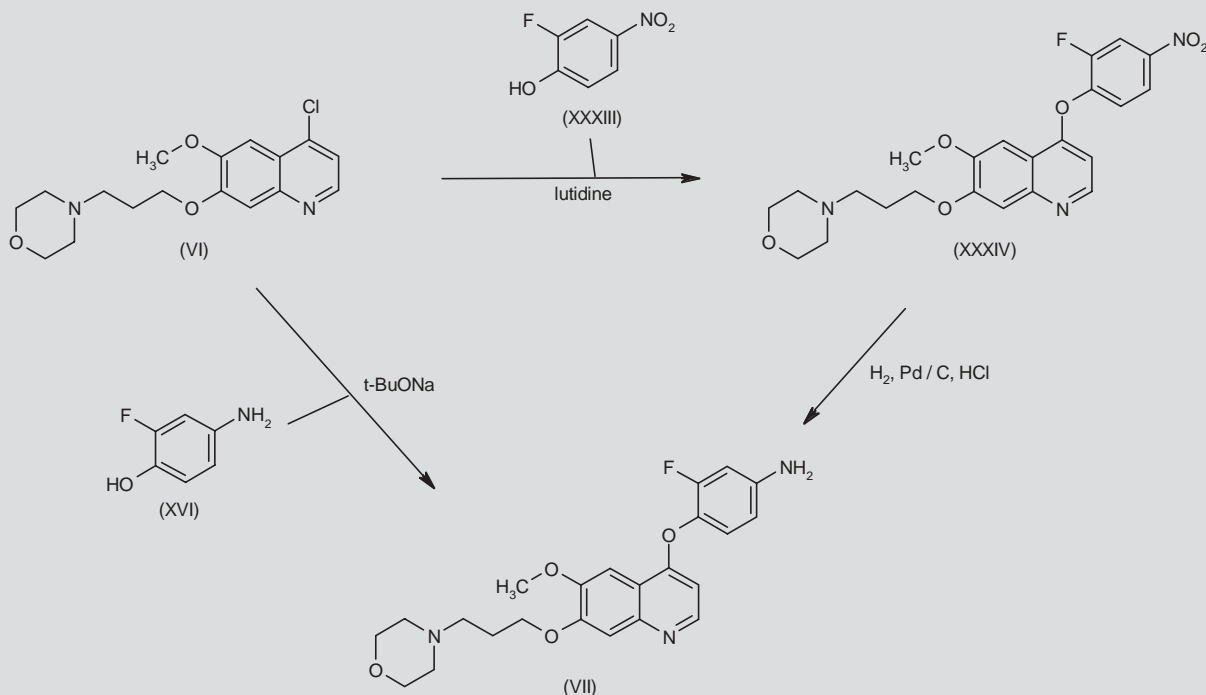
Foretinib is one such multikinase inhibitor that effectively inhibits multiple RTKs, including c-Met, VEGFR-2, MSP receptor and AXL, and to a lesser extent, PDGF-R- $\beta$ , c-Kit and FLT-3 (21). Kinetic studies demonstrate that foretinib reversibly binds in the ATP pocket of the c-Met kinase active site as a competitive inhibitor, while the crystal structure of foretinib bound to c-Met shows that the drug binds both to the ATP pocket and to an adjacent pocket through hydrogen

**Scheme 4.** Synthesis of Intermediate (VI)

bonds and extensive hydrophobic interactions. The molecule displaces a phenylalanine residue to disrupt the catalytic machinery of the protein, and is sequestered from surrounding solvent, enhancing its binding affinity for the receptor. Through this mechanism, foretinib inhibits HGF-induced phosphorylation of c-Met and downstream signaling pathways, such as extracellular signal-regulated kinase (ERK) phosphorylation.

By simultaneously targeting c-Met in tumor cells and VEGFR-2 in vascular epithelial cells, foretinib can prevent tumor growth directly by inhibiting tumor cell proliferation, invasion and metastasis, but also indirectly by preventing the host vascular response and angiogenesis. The ability of foretinib to inhibit a broad spectrum of other RTKs with lower potency may also contribute to its antivasculature activity (21).

**Scheme 5.** Synthesis of Precursor (VII)



## PRECLINICAL PHARMACOLOGY

In vitro studies of foretinib have shown it to potently and robustly inhibit c-Met and VEGFR-2 with  $IC_{50}$  values of 0.4 and 0.9 nmol/L, respectively, in a cell-free system using recombinant proteins (21). Kinetic studies have shown that both VEGFR-2 and c-Met have an estimated dissociation half-life of 15 h and a  $K_{MATP}$  value of 2  $\mu$ mol/L, and that these kinetic constants are indicative of tight, robust binding of foretinib to the receptors. A broad spectrum of cell lines has been screened to assess the cytotoxicity of foretinib. Cytotoxicity is only seen in cell lines with high expression levels of foretinib target proteins, with 73% of the most sensitive cell lines tested found to express very high levels of at least one target receptor.

Murine melanoma B16F10 cell lines with *MET* amplification have been used to evaluate the inhibitory activity of foretinib in vitro. Foretinib was shown to inhibit c-Met in B16F10 cells with an  $IC_{50}$  of 21 nmol/L. It also inhibited c-Met activity in prostate cancer PC-3 cells and VEGFR-2 phosphorylation, a marker for receptor activation, in human umbilical vein endothelial cells (HUVECs) with  $IC_{50}$  values of 23 and 16 nmol/L, respectively (21). B16F10 cell lines were also used to study the ability of foretinib to inhibit HGF-stimulated cell migration and proliferation. Foretinib was shown to block migration of the cells in a Boyden transwell assay and blocked anchorage-independent tumor cell growth.

The conditioned medium from B16F10 cells and breast carcinoma MDA-MB-231 cells stimulates tubule formation in human lung microvascular endothelial (HMVEC-L) cells, a model system used to

study microvascular pathobiology, and this activity was potentially inhibited by foretinib with an  $IC_{50}$  of 4-5 nmol/L (21). These studies also found that foretinib shows little cytotoxicity in endothelial cells, demonstrating that its effects on tubule formation are due to antiangiogenic activity rather than cytotoxicity. Additionally, HMVEC-L cell migration induced by HGF or VEGF was inhibited with  $IC_{50}$  values of 17 and 5 nmol/L, respectively.

A single oral dose of 100 mg/kg of foretinib administered to naive mice inhibited phosphorylation levels of c-Met in liver cells and VEGFR-2 phosphorylation in lung cells for a period of 24 h. Foretinib shows broad and potent inhibition of tumor growth in vivo. In a subcutaneous model of B16F10 melanoma, a single dose also substantially inhibited phosphorylation of c-Met in the primary tumor for 24 h compared to vehicle-treated controls (21). To compare the activity of foretinib against primary and metastatic tumors, a model of lung metastasis was used in which B16F10 cells were implanted into mice via tail vein injection, which subsequently formed malignant nodules in the lung (22). A once-daily dose of foretinib produced a dose-dependent reduction of metastatic tumor burden of 31% and 62%, respectively, at doses of 30 and 100 mg/kg (21). The lung surface tumor burden, which takes into account the total nodule count and average nodule diameter, was also reduced by 50% and 58%, respectively, after treatment with doses of 30 and 100 mg/kg of foretinib. Foretinib treatment of mice with B16F10 solid tumors led to a dose-dependent decrease in primary tumor growth of 64% and 87%, respectively, at 30 and 100 mg/kg. The results demonstrate the potential ability of foretinib to both block the growth of a primary

tumor and to prevent implantation of metastatic cells and the invasion of tissues surrounding the metastatic lesion. This study also provided an indication of the tolerability of foretinib, as the treated groups had no significant reduction in body weight.

In addition to primary tumors and metastatic lesions, foretinib has been shown to be particularly useful in targeting cells resistant to EGFR kinase inhibitors. c-Met amplification has been found in lung adenocarcinoma cells with acquired resistance to tyrosine-protein kinase erbB-1 inhibitors such as gefitinib (23). The lung adenocarcinoma cell line NCI-H820 has been used in pharmacological studies of foretinib activity for inhibiting the growth of tumor cells resistant to erbB-1 inhibitors. These cells overexpress c-Met and also express both a drug-resistant mutation and a drug-sensitive mutation in *EGFR*. The growth of NCI-H820 cells was inhibited by treatment with foretinib alone in the nanomolar range, whereas human lung adenocarcinoma PC-9 cells which lack the *MET* amplification are insensitive to foretinib. *MET* amplification has been found to activate erbB-3 signaling in non-small cell lung cancer HCC827 cells (24), mediating phosphoinositide 3-kinase activity, which promotes cell survival. erbB-3 phosphorylation was strongly inhibited by foretinib in NCI-H820 cells, and signaling through this pathway was shown to be dependent on c-Met using siRNA that specifically knocks down *MET* expression (23). Inhibition of c-Met by foretinib may therefore prevent erbB-3 signaling and result in a reduction in cell survival and growth. Foretinib reduces the growth of NCI-H820 cells more effectively than siRNA, and this may demonstrate the advantages of foretinib as a multikinase inhibitor, as it targets other receptors in addition to c-Met that also affect cell viability.

Foretinib also inhibits AXL, an RTK which is amplified in several cancers, including gastric (25), lung (26) and ovarian cancers (27). A recent study demonstrated that AXL is upregulated in human breast carcinoma BT-474 cell line clones selected for resistance to the erbB-1/erbB-2 inhibitor lapatinib by chronic exposure to the drug (28). Similar to *MET* amplification in gefitinib-resistant lung cancer, AXL amplification was shown to be a mechanism of resistance to lapatinib. Foretinib restored sensitivity of the BT-474-J4-resistant clones to lapatinib by inhibiting AXL ( $IC_{50} = 11$  nmol/L). AXL phosphorylation, indicative of receptor activation, is inhibited by 0.01  $\mu$ mol/L foretinib, and this reduces ERK phosphorylation. By inhibiting AXL activation, foretinib increased apoptosis, as indicated by increased DNA fragmentation and caspase-3/7 activation in BT-474-J4 cells when combined with lapatinib.

## PHARMACOKINETICS AND METABOLISM

The pharmacokinetic properties of foretinib were studied by analysis of blood samples from patients taking part in the phase I clinical trial both before and in the 72 h following the first dose of the trial. To study the accumulation of foretinib in blood plasma following multiple doses, samples were also taken in the 96 h following the fifth daily dose on day 8. The time taken for plasma foretinib concentrations to reach the maximum level was calculated to be 4 h, independent of dose (29). At the maximum tolerated dose (MTD) of 3.6 mg/kg, the peak plasma concentrations for day 1 and day 8 were 90.5 and 218 ng/mL, respectively. The pharmacokinetics of foretinib were not affected by patient age, sex or body weight. Foretinib was found to have a long plasma half-life, with the average value found

to be 40 h for samples taken on both day 1 and day 8. As foretinib has a long half-life, it remains present in the blood plasma during the 9-day nondosing period of the cycle, but at the end of this nondosing period, foretinib levels in the plasma were very low. This observation suggests that perhaps more frequent administration of a lower dose may potentially be a more effective treatment schedule to ensure continual exposure to the drug. Urine collected in the 24 h following the first dose was used to analyze the renal excretion of the drug. The resulting excretion of intact drug was < 1% of the administered dose over the 24-h period following the first dose.

## SAFETY

The completed phase I clinical trial also determined the safety profile of foretinib in humans. Thirty-nine of the 40 patients in the trial reported at least 1 adverse event, which included hypertension, aspartate aminotransferase (AST) elevation and proteinuria. Reported cases of hypertension were most commonly grade 1 or 2, with one grade 3 case at 1.6 mg/kg and two at 3.6 mg/kg (29). Only one of the 10 patients presenting AST elevation had an event above grade 2. All proteinuria events were grade 1-2 and spontaneously resolved in 6 of the 9 patients affected. Fatigue was a common delayed therapy-related event, and one patient was withdrawn due to grade 2 toxicity. Reversible confusion was seen in 2 patients, 1 of whom reported expressive aphasia and apraxia that settled within 8-12 h on day 3 of the second cycle. This patient had recently completed another trial of cediranib (AZD-2171) for medullary thyroid cancer, and it is unclear if these adverse responses were a result of interactions between foretinib and cediranib. The second reported case of confusion was a patient who had completed therapy with bevacizumab, a VEGF-A-inhibiting antibody, and the chemotherapy treatment FOLFOX for colon cancer 6 weeks prior to receiving foretinib. This patient reported disorientation in the first and third cycles of the trial, but it is again unclear if these symptoms were a result of interaction between foretinib and the previous treatments. Other adverse events, including vomiting, diarrhea, fluid retention and pedal edema, were not limiting and were reversed by reducing the administered dose of foretinib. Three patients were withdrawn from the study due to treatment-related adverse events that included grade 3 elevated lipase, grade 3 tumor hemorrhage and grade 4 hemorrhage into central nervous system metastasis in patients receiving doses of 4.5, 3.6 and 0.4 mg/kg, respectively. Three deaths occurred in the 30 days following the last dose, but these were confirmed both clinically and by imaging studies to be associated not with foretinib but with metastatic cancer progression.

A further phase I trial has been completed with a once-daily schedule of foretinib administration and the MTD for this schedule was defined as 80 mg. This dosing regimen has a similar safety profile to the 5 days on/9 days off schedule discussed above (30).

## CLINICAL STUDIES

A phase I clinical trial to determine the MTD of foretinib and its safety profile has been completed. The study analyzed the plasma pharmacokinetics of foretinib and the safety of the drug, as well as determining its preliminary antitumor activity (29). As previously reported preclinical toxicities were known to be reversible, a 5 days on/9 days off schedule was used for this trial. Patients eligible for participation in the study had to be over 18 years of age with confirmed metasta-



tic or unresectable solid tumors of various types, including papillary renal carcinoma and melanoma, for which there is currently no available therapy. Multiple tumor types were included in this study to assess and compare the activity of foretinib against different tumor types. Exclusion criteria included patients who had received chemotherapy, immunotherapy, radiotherapy or an investigational agent in the 4 weeks prior to beginning the trial. Also excluded were patients who had received radiation to more than 25% of their bone marrow tissue, who were pregnant or lactating, and patients known to have brain metastases or uncontrolled intercurrent illness. Each of the 40 patients in the study received an oral dose of foretinib on day 1 of the first cycle of the trial and were then observed for 72 h to ensure no dose-limiting toxicities (DLTs) were presented. The patients then received once-daily doses on days 4-8 of the first cycle. DLTs were determined by clinical observations over the entire period of treatment and were used to determine the MTD of foretinib. DLTs comprised any adverse event rated of grade 3 or above if nonhematological (i.e., nausea, hypertension), or hematological events of grade 4 or above. Eight groups of three to seven patients received doses in the range of 0.1-4.5 mg/kg and two of the four patients receiving the maximum dose of 4.5 mg/kg reported DLTs including elevated levels of serum aspartate aminotransferase (AST) and lipase. The MTD was therefore defined as the lower dose of 3.6 mg/kg, and the median value of 240 mg across the 14 patients receiving this dose was taken as the recommended dose.

The pharmacodynamics of foretinib were studied by taking biopsies from three patients in the trial, selected for the accessibility of their tumors for the procedure. The samples were analyzed for levels of c-Met, phospho-Met, MSP receptor (a member of the Met RTK family), phospho-MSP and the phosphorylated downstream signaling components ERK and Akt. Analysis found little change in overall c-Met and MSP receptor expression in the patients following foretinib treatment, but phosphorylation of the receptors and downstream ERK and Akt decreased in all three patients compared to controls (29). Proliferation index (assayed by Ki67) decreased and apoptosis (assessed by TUNEL staining) increased in the tumor samples following treatment. The results were all seen following the first cycle of the trial, but apoptosis increased further while proliferation and signaling continued to decrease in a second sample taken from one patient biopsied twice during the trial.

The tumor response to foretinib was assessed during the 30 days following the first dose and then every 8 weeks following the Response Evaluation Criteria in Solid Tumors (RECIST) criteria. Of three patients with confirmed partial responses, two had papillary renal carcinoma for which they had received no prior treatment other than surgery, and received foretinib doses of 0.2 and 3.6 mg/kg, respectively. These partial responses lasted for 12 months and over 48 months, respectively (29). The remaining patient had medullary thyroid carcinoma for which the patient had previously received chemotherapy with doxorubicin and the VEGFR inhibitor cediranib, and partial response lasted 10 months. A further 22 patients in the trial had stable disease for 1-10 months, with an average response duration of 4 months. Two patients were withdrawn from the study due to the discovery of previously unknown brain metastases.

Completed phase II trials include studies of foretinib in patients with squamous cell cancer of the head and neck and metastatic gastric

cancer (31). Current and future phase II trials include patients with papillary renal carcinoma, recurrent or metastatic breast cancer and non-small cell lung cancer.

## CONCLUSIONS

Broad-spectrum RTK inhibitors such as foretinib present a novel approach to targeting tumor cells by inhibiting multiple RTKs that may be coactivated in tumor cells and drive cell growth and proliferation. Foretinib binds to and inhibits the activation of multiple RTKs such as c-Met and AXL that are often upregulated in tumor cells. This inhibition can block cell proliferation, invasive activity and metastasis, three of the hallmarks of cancer progression. Additionally, foretinib can also inhibit VEGF receptors such as VEGFR-2 found on endothelial cells to prevent angiogenesis, which is required for tumor progression. Foretinib has been shown to decrease tumor growth in multiple murine models of solid tumors and metastatic lesions.

Phase I clinical trials have shown foretinib to be tolerable in humans and with some preliminary activity in stabilizing and slowing tumor progression. Several phase II trials currently under way include patients with additional tumor types to provide further information on the efficacy of foretinib. Moving forward, more research is needed to determine biomarkers for response to foretinib and to establish its clinical efficacy in patients who have developed resistance to erbB-1 kinase inhibitors.

## SOURCES

Exelixis, Inc. (US); licensed to GlaxoSmithKline (GB).

## DISCLOSURES

The authors state no conflicts of interest.

## REFERENCES

1. Bannen, L.C., Chan, D.S.-M., Chen, J. (Exelixis, Inc.). *c-Met modulators and methods of use*. EP 1673085, EP 2210607, EP 2213661, JP 2007506777, JP 2010235631, JP 2010235632, WO 2005030140.
2. Gilmer, T.M., Greger, J.G. Jr., Liu, L., Shi, H. (GlaxoSmithKline Inc.). *Method of treating cancer using a cMET and AXL inhibitor and an erbB inhibitor*. US 2009274693, WO 2009137429.
3. Deschamps, N.M., Martin, M.T., Monteith, M.J., Zhou, X. (GlaxoSmithKline Inc.). *Preparation of a quinolinylxydiphenylcyclopropanedicarboxamide*. US 2010081805, WO 010036831.
4. Wilson, J., Zuberi, S., Naganathan, S., Goldman, E., Kanter, J. (Exelixis, Inc.). *Methods of preparing quinoline derivatives*. WO 2010056960.
5. Forsyth, T.P., Mac, M.B., Leahy, J.W., Nuss, J.M., Xu, W. (Exelixis, Inc.). *c-Met modulators and methods of use*. EP 1874759, JP 2008537748, US 2008161305, WO 2006108059.
6. Lai, A.Z., Abella, J.V., Park, M. *Crosstalk in Met receptor oncogenesis*. Trends Cell Biol 2009, 19(10): 542-51.
7. Takaki, Y., Furihata, M., Yoshikawa, C. et al. *Sporadic bilateral papillary renal carcinoma exhibiting C-met mutation in the left kidney tumor*. J Urol 2000, 163(4): 1241-2.
8. Lee, J.H., Han, S.U., Cho, H. et al. *A novel germ line juxtamembrane Met mutation in human gastric cancer*. Oncogene 2000, 19(43): 4947-53.



9. Ma, P.C., Kijima, T., Maulik, G. et al. *c-MET mutational analysis in small cell lung cancer: Novel juxtamembrane domain mutations regulating cytoskeletal functions*. *Cancer Res* 2003, 63(19): 6272-81.
10. Bièche, I., Champème M.H., Lidereau, R. *Infrequent mutations of the MET gene in sporadic breast tumours*. *Int J Cancer* 1999, 82(6): 908-10.
11. Benvenuti, S., Comoglio, P.M. *The MET receptor tyrosine kinase in invasion and metastasis*. *J Cell Physiol* 2007, 213(2): 316-25.
12. Di Renzo, M.F., Olivero, M., Martone, T. et al. *Somatic mutations of the Met oncogene are selected during metastatic spread of human HNSC carcinomas*. *Oncogene* 2000, 19(12): 1547-55.
13. Ferrara, N., Gerber, H.P., LeCouter, J. *The biology of VEGF and its receptors*. *Nat Med* 2003, 9(6): 669-76.
14. Pennacchietti, S., Michieli, P., Galluzzo, M. et al. *Hypoxia promotes invasive growth by transcriptional activation of the met protooncogene*. *Cancer Cell* 2003, 3(4): 347-61.
15. Zhang, Y.W., Su, Y., Volpert, O.V. et al. *Hepatocyte growth factor/scatter factor mediates angiogenesis through positive VEGF and negative thrombospondin 1 regulation*. *Proc Natl Acad Sci U S A* 2003, 100(22): 12718-23.
16. Xin, X., Yang, S., Ingle, G. et al. *Hepatocyte growth factor enhances vascular endothelial growth factor-induced angiogenesis in vitro and in vivo*. *Am J Pathol* 2001, 158(3): 1111-20.
17. Gordus, A., Krall, J.A., Beyer, E.M. et al. *Linear combinations of docking affinities explain quantitative differences in RTK signaling*. *Mol Syst Biol* 2009, 5: 235.
18. Xu, A.M., Huang, P.H. *Receptor tyrosine kinase coactivation networks in cancer*. *Cancer Res* 2010, 70(10): 3857-60.
19. Timofeevski, S.L., McTigue, M.A., Ryan, K. et al. *Enzymatic characterization of c-Met receptor tyrosine kinase oncogenic mutants and kinetic studies with aminopyridine and triazolopyrazine inhibitors*. *Biochemistry* 2009, 48(23): 5339-49.
20. Wedge, S.R., Kendrew, J., Hennequin, L.F. et al. *AZD2171: A highly potent, orally bioavailable, vascular endothelial growth factor receptor-2 tyrosine kinase inhibitor for the treatment of cancer*. *Cancer Res* 2005, 65(10): 4389-400.
21. Qian, F., Engst, S., Yamaguchi, K. et al. *Inhibition of tumor cell growth, invasion, and metastasis by EXEL-2880 (XL880, GSK 1363089), a novel inhibitor of HGF and VEGF receptor tyrosine kinases*. *Cancer Res* 2009, 69(20): 8009-16.
22. Bergers, G., Song, S., Meyer-Morse, N. et al. *Benefits of targeting both pericytes and endothelial cells in the tumor vasculature with kinase inhibitors*. *J Clin Invest* 2003, 111(9): 1287-95.
23. Bean, J., Brennan, C., Shih, J. et al. *MET amplification occurs with or without T790M mutations in EGFR mutant lung tumors with acquired resistance to gefitinib or erlotinib*. *Proc Natl Acad Sci U S A* 104(52): 20932-7.
24. Engelman, J.A., Zejnullahu, K., Mitsudomi, T. et al. *MET amplification leads to gefitinib resistance in lung cancer by activating ERBB3 signaling*. *Science* 2007, 316(5827): 1039-43.
25. Wu, C.W., Li, A.F., Chi, C.W. et al. *Clinical significance of AXL kinase family in gastric cancer*. *Anticancer Res* 2002, 22(2B): 1071-8.
26. Shieh, Y.S., Lai, C.Y., Kao, Y.R. et al. *Expression of axl in lung adenocarcinoma and correlation with tumor progression*. *Neoplasia* 2005, 7(12): 1058-64.
27. Sun, W., Fujimoto, J., Tamaya, T. *Coexpression of Gas6/Axl in human ovarian cancers*. *Oncology* 2004, 66(6): 450-7.
28. Liu, L., Gregor, J., Shi, H. et al. *Novel mechanism of lapatinib resistance in HER2-positive breast tumor cells: Activation of AXL*. *Cancer Res* 2009, 69(17): 6871-8.
29. Eder, J.P., Shapiro, G.I., Appleman, L.J. et al. *A phase I study of foretinib, a multi-targeted inhibitor of c-met and vascular endothelial growth factor receptor 2*. *Clin Cancer Res* 2010, 16(13): 3507-16.
30. LoRusso, P., Eder, J.P., Sherman, L. et al. *Final results of a phase I dose escalation study of the safety and pharmacokinetics of foretinib administered orally daily to patients with solid tumors*. *Mol Cancer Ther* 2009, 8(12, Suppl.): A8.
31. U.S. National Institutes of Health (2010) Search of: Foretinib - List Results - ClinicalTrials.gov. [Online] (Updated 19 July 2010) Available at: <http://clinicaltrials.gov/ct2/results?term=foretinib>. Accessed October 28, 2010.

